


Metabolic sensor O-GlcNAcylation regulates megakaryopoiesis and thrombopoiesis through c-Myc stabilization and integrin perturbation

Sudjit Luanpitpong¹  | Jirarat Poohadsuan¹ | Phatchanat Klaihmon¹ |
Xing Kang¹ | Kantpitchar Tangkiettrakul¹ | Surapol Issaragrisil^{1,2,3}

¹Siriraj Center of Excellence for Stem Cell Research, Faculty of Medicine Siriraj Hospital, Mahidol University, Bangkok, Thailand

²Division of Hematology, Department of Medicine, Faculty of Medicine Siriraj Hospital, Mahidol University, Bangkok, Thailand

³Bangkok Hematology Center, Wattanosoth Hospital, BDMS Center of Excellence for Cancer, Bangkok, Thailand

Correspondence

Sudjit Luanpitpong, PhD, Siriraj Center of Excellence for Stem Cell Research, Faculty of Medicine Siriraj Hospital, Mahidol University, 2 Siriraj Hospital, Bangkokknoi, Bangkok 10700, Thailand.
Email: suidjit@gmail.com

Funding information

Thailand Office of Commission on Higher Education, Grant/Award Number: CHE-RES-RG-49; Thailand Research Fund/National Research Council of Thailand, Grant/Award Number: RSA62080103

Abstract

Metabolic state of hematopoietic stem cells (HSCs) is an important regulator of self-renewal and lineage-specific differentiation. Posttranslational modification of proteins via O-GlcNAcylation is an ideal metabolic sensor, but how it contributes to megakaryopoiesis and thrombopoiesis remains unknown. Here, we reveal for the first time that cellular O-GlcNAcylation levels decline along the course of megakaryocyte (MK) differentiation from human-derived hematopoietic stem and progenitor cells (HSPCs). Inhibition of O-GlcNAc transferase (OGT) that catalyzes O-GlcNAcylation prolongedly decreases O-GlcNAcylation and induces the acquisition of CD34⁺CD41a⁺ MK-like progenitors and its progeny CD34⁻CD41a⁺/CD42b⁺ megakaryoblasts (MBs)/MKs from HSPCs, consequently resulting in increased CD41a⁺ and CD42b⁺ platelets. Using correlation and co-immunoprecipitation analyses, we further identify c-Myc as a direct downstream target of O-GlcNAcylation in MBs/MKs and provide compelling evidence on the regulation of platelets by novel O-GlcNAc/c-Myc axis. Our data indicate that O-GlcNAcylation posttranslationally regulates c-Myc stability by interfering with its ubiquitin-mediated proteasomal degradation. Depletion of c-Myc upon inhibition of OGT promotes platelet formation in part through the perturbation of cell adhesion molecules, that is, integrin- α 4 and integrin- β 7, as advised by gene ontology and enrichment analysis for RNA sequencing and validated herein. Together, our findings provide a novel basic knowledge on the regulatory role of O-GlcNAcylation in megakaryopoiesis and thrombopoiesis that could be important in understanding hematologic disorders whose etiology are related to impaired platelet production and may have clinical applications toward an ex vivo platelet production for transfusion.

KEYWORDS

c-Myc, integrins, megakaryocyte, megakaryopoiesis, O-GlcNAcylation, OGT, platelet, thrombopoiesis

This is an open access article under the terms of the Creative Commons Attribution-NonCommercial License, which permits use, distribution and reproduction in any medium, provided the original work is properly cited and is not used for commercial purposes.

©2021 The Authors. STEM CELLS published by Wiley Periodicals LLC on behalf of AlphaMed Press 2021

1 | INTRODUCTION

Hematopoiesis begins early in embryonic development and continues throughout life to produce various mature, functional cells of distinct lineages comprising the blood system. Hematopoietic stem cells (HSCs) are multipotent stem cells capable of forming all blood lineages, while maintaining the balance between opposing cell fates of self-renewal and differentiation.¹ In the past decades, multiple lineage-specific transcriptional programs and complex signaling pathways implicating in HSC cell fate have been intensively defined.²⁻⁴ However, the roles of posttranslational modifications (PTMs) in hematopoiesis and its transcriptional cascades, particularly through the modulation of metabolic signaling, remain largely an unexplored area.

Metabolic state of HSCs has recently emerged as an important regulator of self-renewal and lineage-specific differentiation. For example, glucose and glutamine utilization toward nucleotide biosynthesis can dictate the erythroid lineage commitment, meanwhile an inhibition of glutamine metabolism would favor myelomonocytic differentiation.⁵ O-GlcNAcylation is an essential PTM that uses UDP-GlcNAc, the final product by hexosamine biosynthetic pathway (HBP), as a donor substrate to be added to proteins by O-GlcNAc transferase (OGT) and removed by O-GlcNAcase (OGA). As HBP integrates flux of amino acids, carbohydrates, fatty acids, nucleotides and energy metabolism, the extent of O-GlcNAcylation generally reflects the global metabolic dynamics in the cells.^{6,7}

Megakaryopoiesis is the process by which HSCs and progenitors differentiate into mature megakaryocytes (MKs) that ultimately produce platelets through a multistage process requiring MK maturation and fragmentation so called thrombopoiesis.⁸ Given that aberrant metabolism affects hematopoiesis,^{5,9} O-GlcNAcylation as a critical nutrient signal might influence hematopoietic cell differentiation and maturation, including megakaryopoiesis and thrombopoiesis. To test this hypothesis, we used small molecule inhibitors and CRISPR/Cas9 manipulation of OGT and OGA cycling enzymes to modify cellular O-GlcNAcylation in human umbilical cord blood (UCB)-derived CD34⁺ hematopoietic stem and progenitor cells (HSPCs) and human megakaryoblastic (MB) cell lines that can be induced to undergo MK differentiation and produce platelets. When O-GlcNAcylation is inhibited via OGT inhibition, HSPCs undergo faster MK maturation and produce more functional platelets when compared with control. Induction of platelet production upon OGT inhibition was validated in MB cell models. We further provide molecular insight into: (a) how O-GlcNAcylation controls MKs and platelet release and (b) how it broadly affects biological processes that likely promote the megakaryopoiesis and thrombopoiesis. Our findings provide a novel basic knowledge on the regulatory role of O-GlcNAcylation in megakaryopoiesis and thrombopoiesis that may have clinical utility toward an ex vivo platelet production for transfusion.

2 | MATERIALS AND METHODS

2.1 | Subjects and ethics statement

This study was approved by the Siriraj Review Board (#Si 564/2018 and #Si 090/2020) and was in accordance with the Helsinki

Significance statement

This study reveals that cellular O-GlcNAcylation levels decline along the course of megakaryocyte (MK) differentiation from human-derived hematopoietic stem and progenitor cells. Under normal conditions, O-GlcNAcylation stabilizes c-Myc by interfering with its ubiquitin-mediated proteasomal degradation. Inhibition of O-GlcNAc transferase (OGT) disrupts the c-Myc O-GlcNAcylation, resulting in c-Myc degradation and subsequent integrin perturbation and platelet production. Therefore, inhibition of OGT and O-GlcNAcylation, which could be achieved by small molecule inhibition or genetic manipulation, may hold potential for future clinical applications as a means to improve MK differentiation and platelet production.

Declaration of 1975. UCB were collected from healthy newborns at birth after informed consent from their mothers.

2.2 | Purification of CD34⁺ HSPCs

Mononuclear cells were enriched from human UCB samples over Ficoll-Hypaque gradient (GE Healthcare, UK) and CD34⁺ HSPCs were subsequently isolated using CD34 MicroBead Kit and MS Column (Miltenyi, Germany) according to the manufacturer's protocol. The purity was approximately 90% as evaluated by flow cytometry (BD Biosciences).

2.3 | In vitro cultures of MKs from CD34⁺ cells

CD34⁺ cells isolated from UCB samples were expanded for 3 days in IMDM medium (Gibco) supplemented with 10% fetal bovine serum (FBS) (Merck Millipore, Germany) and 25 ng/mL each of recombinant human (rh) SCF, rhIL-3, rhIL-6 and rhFlt3-L (Miltenyi, Germany). MK medium was MegaCult-C (STEMCELL Technologies, Canada) consisted of IMDM supplemented with bovine serum albumin, insulin, transferrin, 2-mercaptoethanol, rhTPO, rhIL-6, and rhIL-3.

2.4 | Cell culture

MEG-01 and its subclone MEG-01s MB cell lines were obtained from JCRB Cell Bank (Japan), cultured in RPMI1640 medium (Gibco) with 10% FBS and maintained in a humidified atmosphere of 5% CO₂ environment at 37°C.

2.5 | Characterization of MKs and platelet-like particles

Cultured cells were characterized by incubating with APC-conjugated anti-human CD34, APC-Cy7-conjugated CD41a, PE-conjugated

CD42b, FITC-conjugated anti-Annexin V and/or PE-conjugated CD62P antibodies for 15 minutes at room temperature and analyzed using FACScalibur flow cytometer (BD Biosciences, San Jose, California). Cells and platelet-like particles (PLPs) were defined using the forward (FSC) and side scatter (SSC). Absolute counts were performed using BD Trucount tubes.

2.6 | Platelet aggregation

Platelets were precipitated from culture by 2-step centrifugation at 160g for 10 minutes and 1100g for 15 minutes. The pellets were resuspended and transferred into the 96-well plate and thrombin (10 U/mL) was added to induce the aggregation. Aggregates were stained for F-actin using Alexa Fluor 488 phalloidin and visualized by fluorescence microscopy (Eclipse Ti-U, Nikon, Tokyo, Japan).

2.7 | CRISPR/Cas9 and shRNA-mediated gene knockdown

For CRISPR/Cas9 system, all-in-one lentiviral plasmids carrying SpCas9-puromycin resistance and sgRNA sequences against human *OGT*, *MGEA5*, *ITGB7* and *ITGA4* were obtained from GenScript, while retroviral plasmid carrying shRNA sequences against human *MYC* was a kind gift from Prof. Martin Eilers (Addgene #29435).¹⁰ Viral particles were transduced into the MKs in the presence of hexadimethrine bromide (8 µg/mL) for 48 hours. The cells were then selected with puromycin (1 µg/mL) and analyzed for protein levels by Western blotting prior to use.

2.8 | Western blot analysis

Cell were incubated in a commercial lysis buffer (Cell Signaling Technology) and a protease inhibitor mixture (Roche Molecular Biochemicals) at 4°C for 30 minutes. Protein content was analyzed using BCA protein assay (Pierce Biotechnology) and 50-150 mg of proteins were resolved under denaturing conditions by SDS-PAGE and transferred onto PVDF membranes. Membranes were blocked with 5% nonfat dry milk, incubated with appropriate primary antibodies at 4°C overnight and subsequently incubated with peroxidase-conjugated secondary antibodies for 1 hour at room temperature. The immune complexes were analyzed by enhanced chemiluminescence detection system on a digital imager ImageQuant LAS (GE Healthcare).

2.9 | O-GlcNAcylation and ubiquitination

Cell lysates (200 µg) were immunoprecipitated by incubating with Dynabeads Protein G magnetic beads (Invitrogen) conjugated with anti-c-Myc antibody for 30 minutes at room temperature. The immune

complexes were washed four times, resuspended in 2× Laemmli sample buffer, separated by SDS-PAGE and analyzed for O-GlcNAcylation or ubiquitination using anti-O-GlcNAc (RL2) or anti-ubiquitin antibody (Santa Cruz Biotechnology), respectively. EasyBlot anti-mouse or anti-rabbit IgG (GeneTex), which is a horseradish peroxidase (HRP)-conjugated secondary antibody, were employed to avoid the interference from heavy and light chains of antibodies in immunoprecipitation assays.

2.10 | RNA sequencing and data analysis

Total RNA was extracted using Total RNA Purification Kit (GMBiolab, Taiwan). mRNA enrichment, library construction, sequencing on an Illumina NovaSeq6000 (San Diego, California) and differential expression analysis were performed by Novogene (Beijing, China) (GEO accession number: GSE150880). Downstream analysis was performed using a combination of programs including STAR (v2.5) with hg19 as reference genome, HTSeq (v0.6.1), Cufflink and Novogene's wrapped scripts. Alignments were parsed using Tophat program and differential gene expressions (DEGs) were determined through DESeq2. DESeq2 provides statistical routines of *P*-value, which were adjusted by Benjamini and Hochberg's approach for controlling the false discovery rate. Genes with an adjusted *P*-value <.05 were assigned as differentially expressed. Gene ontology and enrichment analysis was performed using Database for Annotation, Visualization and Integrated Discovery Bioinformatics Resources (DAVID v6.8), as a comprehensive set of functional annotation tools. Protein-protein interaction of differentially expressed genes was based on the Search Tool for Retrieval of Interacting Genes/Proteins (STRING) database and Cytoscape software (v3.7.2) was used for data integration and visualization.

2.11 | RNA isolation and quantitative real-time PCR analysis

Total RNA was prepared using TRIzol reagent (Invitrogen) and cDNA was prepared using SuperScript III rst-strand synthesis system and oligo (dT) primers (Invitrogen). Quantitative real-time PCR (qPCR) analysis was carried out on a 7500 Fast real-time PCR using a Power SYBR Green PCR master mix (Applied Biosystems). Initial enzyme activation was performed at 95°C for 10 minutes, followed by 40 cycles of denaturation at 95°C for 15 seconds and primer annealing/extension at 60°C for 1 minute. Relative expression of each gene was normalized against the housekeeping *GAPDH* gene product.

2.12 | Statistical analysis

The data represent means ± SD from three or more independent experiments. Statistical analysis was performed by two-sided Student's *t* test or one-way ANOVA followed by a Bonferroni posttest at a significance level of *P* < .05.

3 | RESULTS

3.1 | Global O-GlcNAcylation level declines along MK differentiation from UCB-derived CD34⁺ HSPCs

First, we induced the commitment of CD34⁺ cells to MK lineage by culturing them in specialized medium and profiled immunophenotypic

kinetics of HSPC marker CD34 and MK markers CD41a and CD42b. Flow cytometry plots in Supporting Information Figure S1 shows that an expression of CD34 substantially decreased during differentiation time course as opposed to an observed increase in CD41a and CD42b expression. The great amount of differentiated cells after 10 days of differentiation were CD41a⁺ MBs/MKs, mostly (>80%) with CD34⁻ and some with CD42b⁺ (~25%). The precise percentage of different

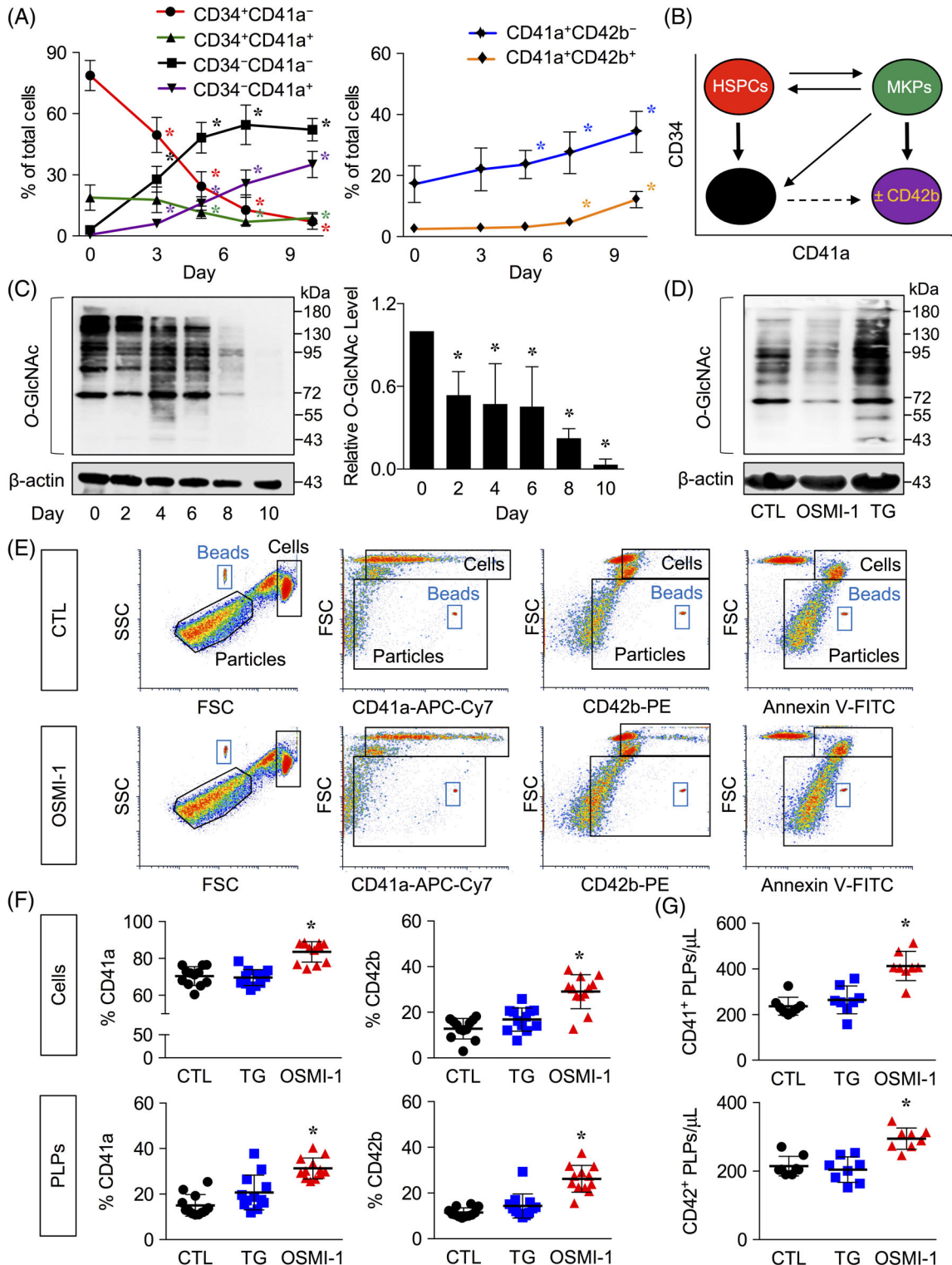


FIGURE 1 Legend on next page.

subpopulations were summarized in Figure 1A. To further identify the true MK progenitors (MKPs) herein, we sorted the differentiated cells at day 3 into CD34⁺CD41a⁺ and CD34⁻CD41a⁻ cell fractions, separately cultured them in MK medium and reanalyzed for CD34 and CD41a expression at various times. We demonstrated that MKP-like cells were essentially found in CD34⁺CD41a⁺, but not CD34⁻CD41a⁻, cell fraction, as evidenced by a remarkably rise of CD34⁻CD41a⁺ MBs/MKs only from this fraction (~40% vs ~5% at day 7 of culture) (Supporting Information Figure S2). Surprisingly, we detected a decent amount (~10%) of CD34⁺CD41a⁻ cells from CD34⁺CD41a⁺ culture, suggesting dynamics toward HSPCs, which required further investigations. The overall process of MK differentiation occurred in this specialized culture were illustrated in Figure 1B, while the growth curves of total cells and different subpopulations were shown in Supporting Information Figure S3.

To explore the potential role of O-GlcNAcylation in MK differentiation, we analyzed the cellular O-GlcNAcylation during differentiation time course by Western blotting using an O-GlcNAc-specific antibody (RL2). Figure 1C shows that O-GlcNAcylation level significantly decreased at day 2 of culture and gradually declined along the course of differentiation, associating with the decrease in OGT enzyme level (Supporting Information Figure S4) and supporting the involvement of O-GlcNAcylation in the process.

3.2 | Inhibition of OGT and O-GlcNAcylation induces MK differentiation and platelet production

During differentiation, MKs grow in size and release platelets, referred to as cellular dust, from their cytoplasm upon maturation.¹¹ To extensively elaborate the effects of O-GlcNAcylation on MK differentiation and subsequent platelet production, we adopted the flow cytometric analysis using FSC and SSC to distinguish between cells and particles, designated as PLPs, based on discrepancy in size¹² together with MK markers CD41a and CD42b and cellular apoptosis/proplatelet marker

Annexin V. We manipulated O-GlcNAcylation through an inhibition of OGT that caused a decrease in global O-GlcNAcylation and an inhibition of OGA that caused an increase in O-GlcNAcylation using small molecule inhibitors OSMI-1 and thiamet G, respectively (Figure 1D and Supporting Information Figure S5). Following the gating strategy shown in Figure 1E, we found that a single treatment of OGT inhibitor OSMI-1 (5 μ M) at the start of culture (day 0) significantly increased subpopulations of CD41a⁺ and CD42b⁺ cells at 10 days after differentiation when compared with nontreated control (Figure 1F, upper), indicating a more MB/MK-like cells upon OGT inhibition. The low percentage of Annexin V⁺ cells in all groups ensured the non-cytotoxicity of the inhibitors (Supporting Information Figure S6, left). Next, we estimated the platelet release from MKs in culture by a calculation of PLPs that were positive for CD41a⁺ and CD42b⁺ from the total events of CD41a⁺ and CD42b⁺ and reported as percentage of CD41a⁺ PLPs and CD42b⁺ PLPs in Figure 1F (lower). Both CD41a⁺ and CD42b⁺ PLPs were found to be substantially increased by OSMI-1 by approximately 3-fold at day 10 when compared with control, indicating a platelet induction upon OGT inhibition. With a low basal level of PLPs in culture, it is not surprising that the inhibitory role of OGA inhibition by thiamet G (10 μ M) in platelet production was not observed herein. Notably, there was no significant difference in Annexin V expression in PLPs in all groups (Supporting Information Figure S6, right).

Absolute platelet counts revealed an increase in the number of CD41a⁺ PLPs and CD42b⁺ PLPs (Figure 1G), thereby validating the platelet promoting role of OGT inhibition by OSMI-1. To rule out whether an increase in total platelets was due to an increase in cell proliferation, we performed total MB/MK counts at day 10 where PLPs were detected. Supporting Information Figure S7A,B demonstrated that OSMI-1 had minimal effect on overall cell growth. Hence, we postulated that OSMI-1 stimulated platelet production through MK maturation, as preliminary supported by a remarkable increase in the more mature CD42b⁺ MBs/MKs upon OSMI-1 treatment at day 10 (Supporting Information Figure S7C).

FIGURE 1 Inhibition of OGT induces MK differentiation and platelet production from UCB-derived HSPCs. A, UCB-derived HSPCs were cultured in specialized MK medium and HSPC marker CD34 and MK markers CD41a and CD42b were analyzed at various times of culture (day 0–day 10) by flow cytometry. Percentage of different subpopulations, including CD34⁺CD41a⁻, CD34⁺CD41a⁺, CD34⁻CD41a⁻, and CD34⁻CD41a⁺ cells as well as CD41a⁺CD42b⁻ and CD41a⁺CD42b⁺ MB/MK-like cells were shown. Data are mean \pm SD (n = 6) from six independent experiments. *P < .05 vs cells at the day of differentiation (day 0); two-sided Student's t test. Representative flow cytometry plots of CD34 and CD41a as well as CD41a and CD42b were shown in Supporting Information Figure S1. B, Schematic pathways for the acquisition of CD41a and CD42b surface antigens from CD34⁺ HSPCs. Dashed line indicates a possible minor pathway. C, (left) Cellular O-GlcNAcylation was evaluated along the course of MK differentiation by Western blotting using anti-O-GlcNAc-specific antibody (RL2). Blots were reprobed with anti- β -actin antibody to confirm equal loading of the samples. (right) Quantitative analysis of O-GlcNAcylation level by densitometry is shown. Data are mean \pm SD (n = 3) from three independent experiments. *P < .05 vs cells at day 0; two-sided Student's t test. D–G, CD34⁺ HSPCs were treated with thiamet G (TG; 10 μ M), OSMI-1 (5 μ M) or left untreated (CTL) at day 0. D, Cellular O-GlcNAcylation of different groups after 10 days of differentiation (day 10) was evaluated by Western blotting using anti-O-GlcNAc-specific antibody (RL2) (see also Supporting Information Figure S5 for quantitative analysis). E, Flow cytometry gating strategy using FSC vs SSC to distinguish MKs/MBs (cells) and platelets (particles; PLPs) based on size and analysis of CD41a, CD42b and Annexin V at day 10. F, (upper) Percentage of CD41a⁺ and CD42b⁺ cells from total events. (lower) Percentage of CD41a⁺ and CD42b⁺ PLPs from total positive events. Data are mean \pm SD (n = 12) from 12 independent experiments. *P < .05 vs nontreated control (CTL); two-sided Student's t test. Percentage of Annexin V⁺ cells and PLPs was shown in Supporting Information Figure S6. G, Absolute numbers of CD41a⁺ and CD42b⁺ PLPs at day 10 were determined by comparing PLP events to Trucount bead events using flow cytometric analysis. Data are mean \pm SD (n = 8) from eight independent experiments. *P < .05 vs CTL; two-sided Student's t test

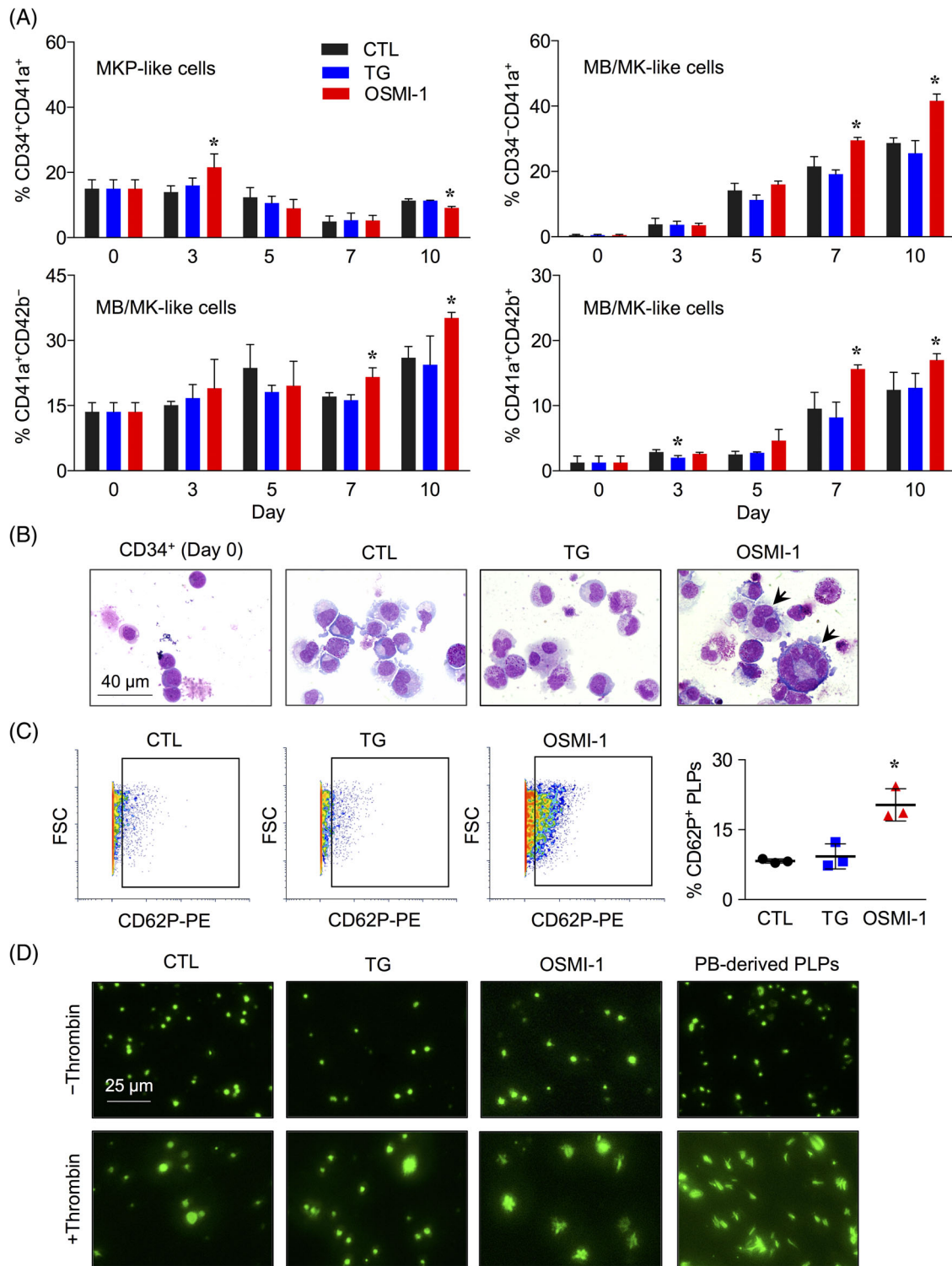


FIGURE 2 Inhibition of OGT promotes MK maturation and yields normal function platelets. A, CD34⁺ HSPCs were treated with thiamet G (TG; 10 μ M) or OSMI-1 (5 μ M) and were analyzed for CD34, CD41a and CD42b expression at day 3, day 5, day 7 and day 10 of culture. Percentage of CD34⁺CD41a⁺ MKP-like cells and CD34⁻CD41a⁺, CD41a⁺CD42b⁻ and CD41a⁺CD42b⁺ MB/MK-like cells were shown. Data are mean \pm SD (n = 3) from three independent experiments. *P < .05 vs nontreated control (CTL) at the same day; two-sided Student's t test. B, Representative morphology of CD34⁺ HSPCs at the day of differentiation (day 0) and cultured cells of different groups at day 10 on Wright-stained cytopsin slides. Arrows indicate multinucleated cells with protrusions. Scale bar = 40 μ m. Additional micrographs from multiple, independent experiments can be found in Supporting Information Figure S9. C, Flow cytometric analysis of CD62P in precipitated PLPs at day 10. Plots are percentage of CD62P⁺ PLPs from total PLPs. Data are mean \pm SD (n = 3) from three independent experiments. *P < .05 vs CTL; two-sided Student's t test. D, Platelet aggregation in different groups was induced by thrombin in comparison to PB-derived PLPs. Aggregates were stained for F-actin using Alexa Fluor 488 phalloidin to aid the visualization. Scale bar = 25 μ m. Quantitative analysis of aggregate size was shown in Supporting Information Figure S10

3.3 | Inhibition of OGT promotes MK maturation

Having demonstrated that CD34⁺CD41a⁺ subpopulation was MKP-like cells (Supporting Information Figure S2), we evaluated the effect of OGT inhibition by OSMI-1 on the acquisition of CD34⁺CD41a⁺ cells during early differentiation time course. Figure 2A and Supporting Information Figure S8 shows that there was a substantial higher percentage of CD34⁺CD41a⁺ MKPs upon OSMI-1 treatment when compared with control at day 3. OSMI-1 group started to show a higher CD34⁺CD41a⁺, CD41a⁺CD42b⁻, and CD41a⁺CD42b⁺ MB/MK-like cells at day 7 onwards. Consistently, morphological appearance of OSMI-1-treated cells by Wright-stained cytospin exhibited more mature MK phenotypes, for example, large size, multinucleated cells with protrusions, when compared with control at day 10 (Figure 2B and Supporting Information Figure S9, arrows). Differences in O-GlcNAcylation level as modulated by thiamet G or OSMI-1 at day 0 remained even after 10 days of differentiation when compared with nontreated control (Figure 1D and Supporting Information Figure S5), suggesting that O-GlcNAcylation plays a part throughout early and late MK differentiation and maturation.

3.4 | Platelets induced by OGT inhibition display normal function

CD62P, also known as surface P-selectin, is an important marker for platelet activation and release reaction.¹³ Total PLPs precipitated from the culture at day 10 were analyzed for CD62P expression by flow cytometry. Figure 2C shows that OSMI-1-treated cells released remarkable higher percentage of CD62P⁺ PLPs even at native state, suggesting that OSMI-1-induced PLPs were readily primed for an activation. To identify whether OGT inhibition by OSMI-1 interfered with platelet function, PLPs were next activated by thrombin to induce an aggregation. The results showed that PLPs derived from all groups could form big aggregates upon activation similar to that of peripheral blood (PB)-derived platelets (Figure 2D and Supporting Information Figure S10).

3.5 | Inhibition of OGT similarly induces platelets in MB cell lines

Due to limitations in cell number and case-to-case variations of CD34⁺-derived MKs, human-derived MB MEG-01 and MEG-01s cells¹⁴ were used to further investigate the mechanisms behind platelet production. We used valproic acid (VPA), an efficient agent for platelet induction in MEG-01 cells,¹⁵ to first generate the cellular and PLP profile. Using similar gating strategy as CD34⁺-derived MKs (Figure 3A), we found that the percentage of CD41a⁺ and CD42b⁺ cells appeared to be reduced as opposed to an increase in CD41a⁺ and CD42b⁺ PLPs upon platelet induction (Figure 3B), suggesting that PLPs were produced by shedding from the cells through the ruptures of cytoplasm.

To determine the direct relationship between O-GlcNAcylation level and platelet induction, MEG-01 cells were treated with various concentrations of noncytotoxic OSMI-1 (0–20 μM) and thiamet G (0–15 μM) and their effects on CD41a⁺ and CD42b⁺ cells and PLPs were determined. Figure 3C shows that OGT inhibitor OSMI-1 significantly induced CD41a⁺ PLPs and, to a lesser extent, CD42b⁺ PLPs in a dose-dependent manner in the MEG-01 cells. Consistent with the finding in CD34⁺-derived MKs, OGA inhibitor thiamet G had minimal effects on the CD41a⁺ and CD42b⁺ cells and PLPs, due likely to the low basal PLPs in culture. The inductive effect of OSMI-1 on platelet production, as analyzed by CD41a⁺ and CD42b⁺ PLPs, was confirmed in MEG-01s cells (Figure 3D).

Next, we used CRISPR/Cas9 system to repress OGT and MGEA5 (encoding OGA) in MEG-01 cells to validate the results from small molecule inhibitors to ascertain the roles of O-GlcNAcylation in platelet production (Figure 4A). Figure 4B shows that genetic inhibition of OGT (OGTi) significantly induced CD41a⁺ and CD42b⁺ PLPs when compared with CRISPR/Cas9 control (CTLi), thus confirming that OGT inhibition and subsequent reduction of global O-GlcNAcylation induces platelets in MBs. Due to the low basal PLPs in culture, VPA was used to induce the release of PLPs to evaluate whether genetic inhibition of OGA (OGAi) would suppress PLPs. The VPA-induced CD41a⁺ and CD42b⁺ PLPs was observed to be significantly lower in OGAi cells when compared with CTLi cells (Figure 4C). For consistency, we reevaluated whether OGA inhibition by thiamet G (0–15 μM) could rescue the effects of VPA in MEG-01 cells. Figure 4D indicates that thiamet G significantly suppressed VPA-induced PLPs, similar to those observed in OGAi cells, in a dose-dependent manner. Altogether, these results substantiate the positive regulatory role of OGT inhibition and the opposing role of OGA inhibition in thrombopoiesis through O-GlcNAcylation.

3.6 | O-GlcNAcylation regulates c-Myc level

It has been reported that c-Myc plays essential roles in hematopoiesis, HSC self-renewal and differentiation.^{16,17} Recent evidence suggests that c-Myc should be depleted to permit efficient platelet formation from induced pluripotent stem cell-derived MKs.^{18,19} To elucidate the underlying mechanisms by which O-GlcNAcylation mediates thrombopoiesis, we monitored the level of global O-GlcNAcylation along with the level of c-Myc, a reported target of O-GlcNAcylation in cancers,^{20–22} following OGT and OGA inhibition by OSMI-1 and thiamet G by Western blotting. The level of c-Myc was found to decrease or increase markedly with the level of O-GlcNAcylation in both MEG-01 and MEG-01s cells (Figures 5A–C). Further analysis of the correlation between O-GlcNAcylation and c-Myc in the tested cells reveals the direct relationship of the two events with a very high correlation coefficient ($r = 0.9070$) (Figure 5D), thus indicating that O-GlcNAcylation regulates c-Myc in MB cells. It is worthy to mention that O-GlcNAcylation also correlates well with the level of total YAP (Supporting Information Figure S11), which is a major effector of the Hippo pathway^{23,24} that was previously reported to be involved in

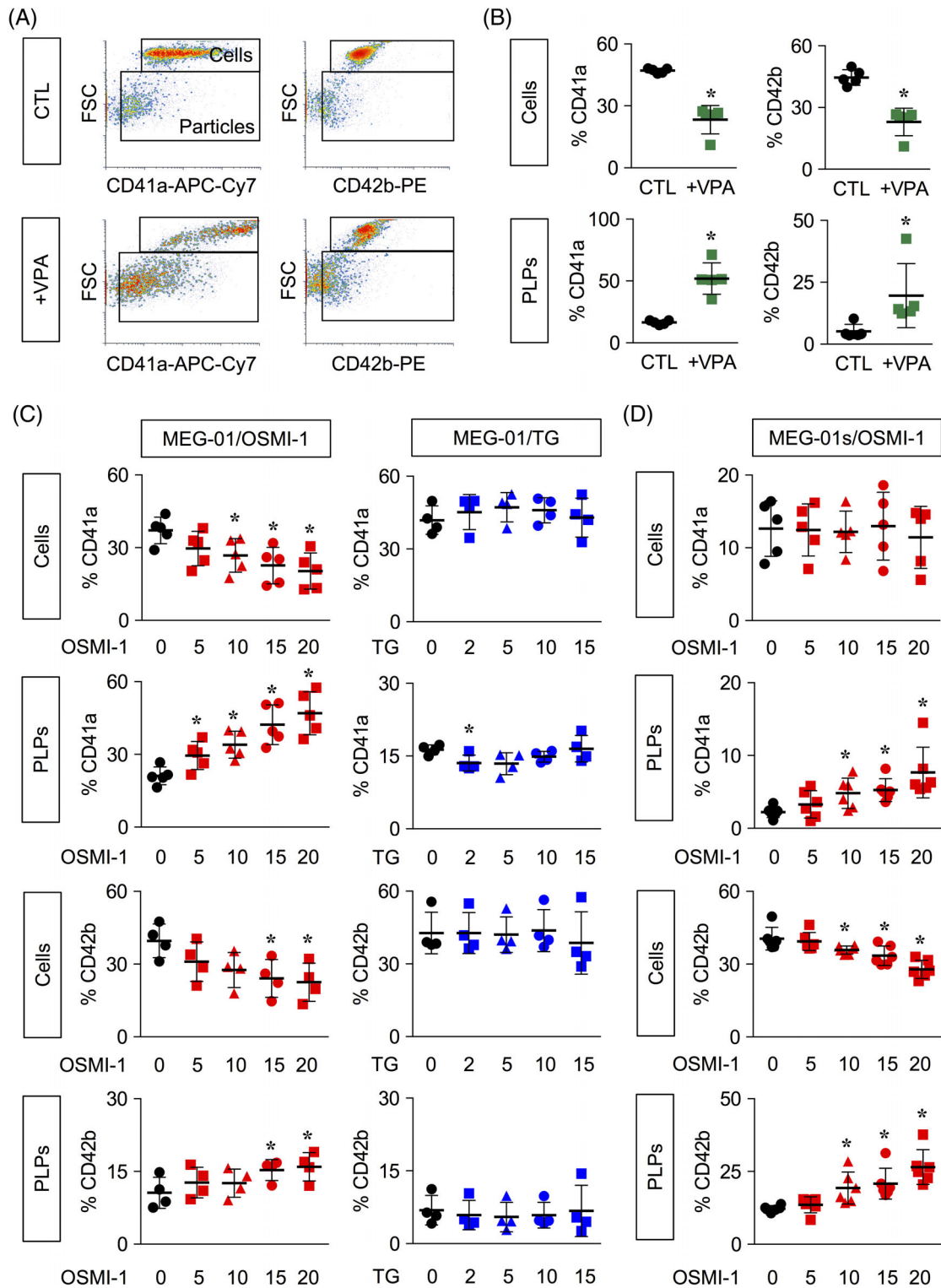


FIGURE 3 Inhibition of OGT dose-dependently induces platelets in MB cells. A, Flow cytometry gating strategy for analysis of CD41a⁺ and CD42b⁺ cells and PLPs in MB MEG-01 and MEG-01s cells, using VPA (2 mM) as a platelet inducer. B, (Upper) Percentage of CD41a⁺ and CD42b⁺ cells from total events. (Lower) Percentage of CD41a⁺ and CD42b⁺ PLPs from total positive events. Data are mean ± SD (n = 5) from five independent experiments. *P < .05 vs nontreated control (CTL); two-sided Student's *t* test. C, MEG-01 cells were treated with various concentrations of OSMI-1 (0-20 μM) or thiamet G (TG; 0-15 μM) for 3 days and percentage of CD41a⁺ and CD42b⁺ cells and PLPs were similarly analyzed by flow cytometric analysis and plotted. Data are mean ± SD (n = 5) from five independent experiments. *P < .05 vs CTL; two-sided Student's *t* test. D, MEG-01s cells were similarly treated with various concentrations of OSMI-1 (0-20 μM) for 3 days and percentage of CD41a⁺ and CD42b⁺ cells and PLPs were analyzed by flow cytometric analysis and plotted. Data are mean ± SD (n = 6) from six independent experiments. *P < .05 vs CTL; two-sided Student's *t* test

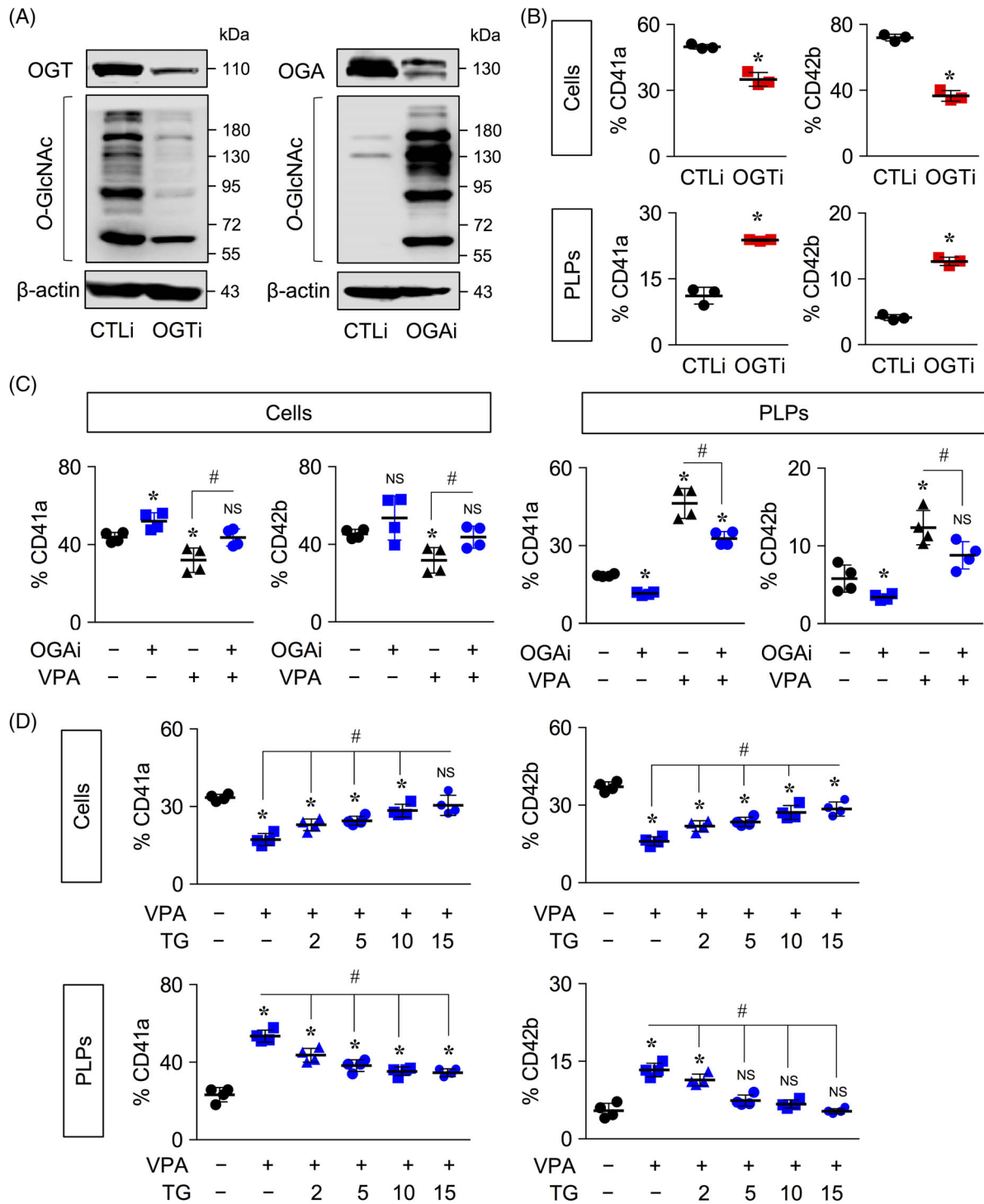


FIGURE 4 Inhibition of OGT and OGA by CRISPR/Cas9 system and their effects on platelet production. A, CRISPR/Cas9 system was used to repress OGT and MGEA5 (encoding OGA) in MB MEG-01 cells, designated as OGTi and OGAI cells, respectively. Western blot analysis of OGT or OGA and cellular O-GlcNAcylation levels in OGTi and OGAI cells in comparison to control (CTLi) cells. B, Flow cytometric analysis of CD41a⁺ and CD42b⁺ cells and PLPs in OGTi and CTLi cells collected at 3 days of culture. Percentage of CD41a⁺ and CD42b⁺ cells from total events (upper) and PLPs from total positive events (lower) were plotted. Data are mean \pm SD (n = 3) from three independent experiments. **P* < .05 vs CTLi cells; two-sided Student's *t* test. C, OGAI cells were treated with or without VPA (2 mM) for 6 days and percentage of CD41a⁺ and CD42b⁺ cells (left) and PLPs (right) were evaluated by flow cytometry and plotted. Data are mean \pm SD (n = 4) from four independent experiments. **P* < .05 vs CTLi cells or PLPs; NS, not significance vs CTLi cells or PLPs; one-way ANOVA with Bonferroni posttest. #*P* < .05 vs VPA-treated CTLi cells or PLPs; NS, not significance vs VPA-treated CTLi cells or PLPs; one-way ANOVA with Bonferroni posttest. D, MEG-01 cells were treated with thiamet G (TG; 0-15 μ M) and similarly treated VPA (2 mM) for 6 days and percentage of CD41a⁺ and CD42b⁺ cells (upper) and PLPs (lower) were evaluated by flow cytometry and plotted. Data are mean \pm SD (n = 4) from four independent experiments. **P* < .05 vs nontreated control (CTL) cells or PLPs; NS, not significance vs CTL cells or PLPs; one-way ANOVA with Bonferroni posttest. #*P* < .05 vs VPA-treated cells or PLPs; one-way ANOVA with Bonferroni posttest

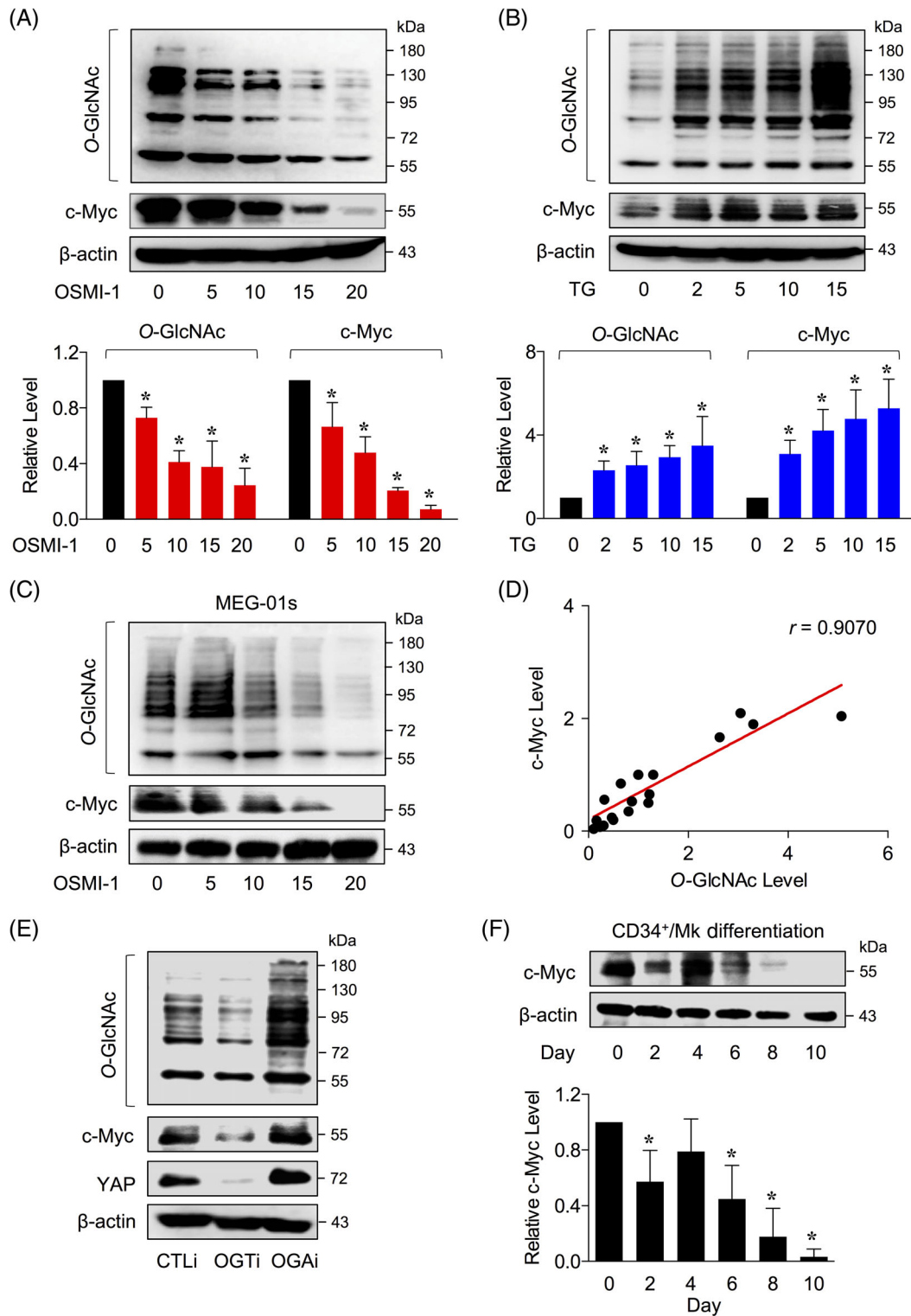


FIGURE 5 Correlation analysis of O-GlcNAcylation and c-Myc. A-D, MEG-01 or MEG-01s cells were treated with OSMI-1 (0-20 μ M) or thiamet G (TG; 0-15 μ M) for 24 hours. A,B, (upper) Western blot analysis of O-GlcNAcylation and c-Myc levels in response to (A) OSMI-1 or (B) TG in MEG-01 cells. (Lower) Quantitative analysis of O-GlcNAcylation and c-Myc levels by densitometry. Data are mean \pm SD ($n = 3$) from three independent experiments. * $P < .05$ vs nontreated control cells; two-sided Student's t test. C, Western blot analysis of O-GlcNAcylation and c-Myc levels in response to OSMI-1 in MEG-01s cells. D, Correlation analysis of O-GlcNAcylation and c-Myc levels in MB MEG-01 and MEG-01s cells. r , correlation coefficient. E, Western blot analysis of O-GlcNAcylation, c-Myc and YAP levels in CTLi, OGTi and OGAI cells to confirm their relationships. F, UCB-derived CD34⁺ HSPCs were cultured in specialized MK differentiation medium. (upper) Western analysis of c-Myc level at various times of culture. (lower) Quantitative analysis of c-Myc levels by densitometry. Data are mean \pm SD ($n = 3$) from three independent experiments. * $P < .05$ vs CD34⁺ cells at the day of differentiation (day 0); two-sided Student's t test

the regulation of platelet-like crystal cells in *Drosophila*²⁵ and human platelets.²⁶ The levels of O-GlcNAcylation, c-Myc and YAP upon genetic inhibition of OGT and OGA were also evaluated and their correlations were similarly observed (Figure 5E), thereby confirming that O-GlcNAcylation acts upstream of c-Myc and YAP in MBs. As c-Myc

was reported to be a direct target of YAP²⁷⁻²⁹ that was under controlled by O-GlcNAcylation in the tested system, we further emphasized on the regulatory axis of O-GlcNAcylation and c-Myc in platelet production. To validate that the regulation of c-Myc by O-GlcNAcylation occurs throughout MK differentiation and

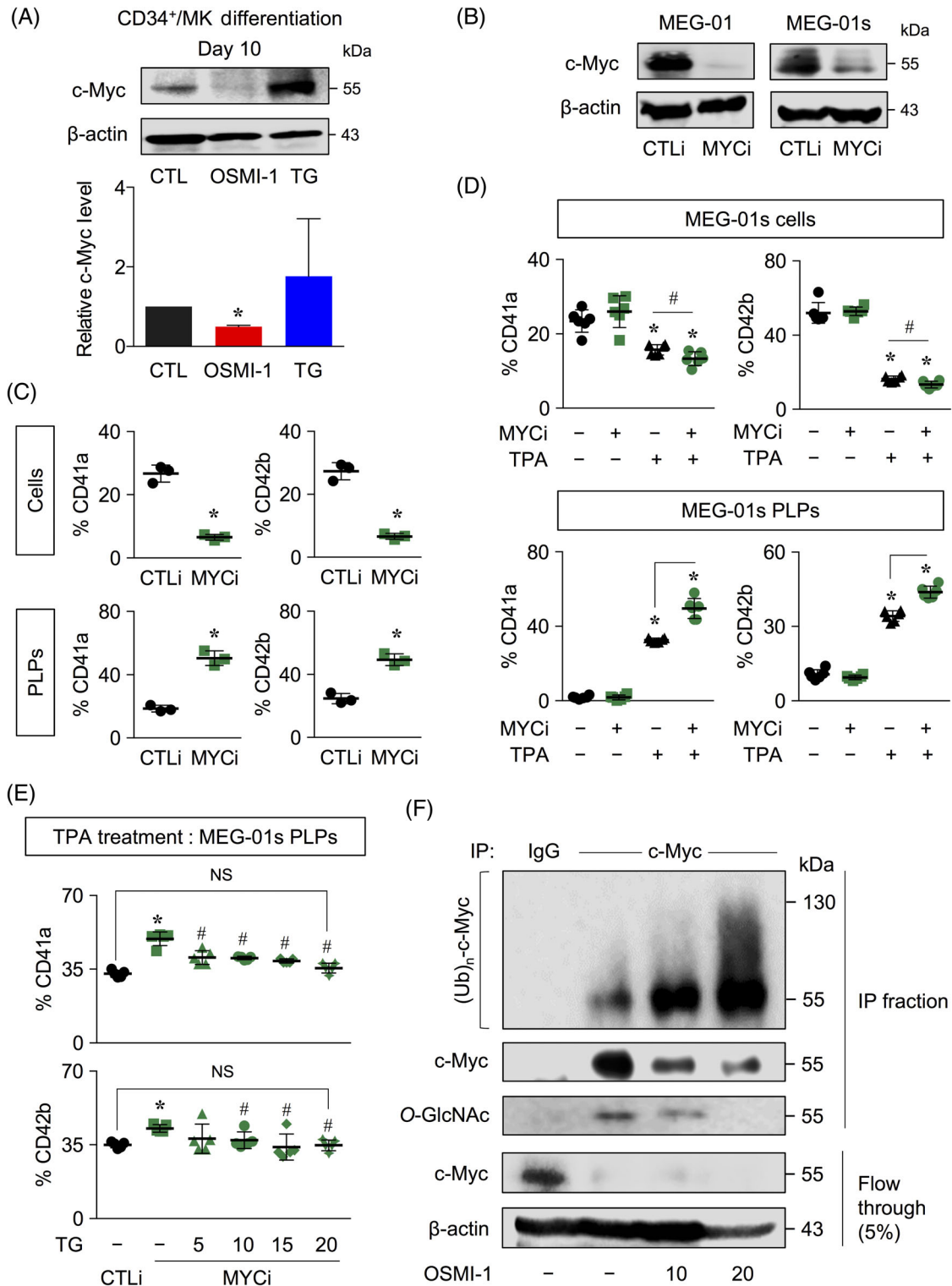


FIGURE 6 Legend on next page.

maturation, we determined the level of c-Myc during the course of CD34⁺ differentiation into MBs/MKs. Figure 5F shows that c-Myc level was high at the day of differentiation (day 0) and gradually declined to the minimum at day 10, in correlation with the decrease in O-GlcNAcylation level (Figure 1C), thus strengthening the involvement of O-GlcNAc/c-Myc axis in the process.

3.7 | O-GlcNAcylation mediates platelet production via c-Myc

During MK differentiation from CD34⁺ HSPCs at day 10, c-Myc was found to be mostly downregulated in OSMI-treated cells, of which produced highest platelets (Figure 6A). To first confirm the role of c-Myc in platelet production, c-Myc expression was inhibited in MEG-01 and MEG-01s cells using shRNA against MYC as shown in Figure 6B. In line with the results from OGT inhibition, CD41a⁺ and CD42b⁺ PLPs were found to be significantly higher upon c-Myc inhibition (MYCi) in MEG-01 cells when compared with control (CTLi) (Figure 6C). Meanwhile, the inductive effect of c-Myc inhibition on CD41a⁺ and CD42b⁺ PLPs in MEG-01s cells was detected when 12-O-tetradecanoylphorbol-13-acetate (TPA), an efficient agent for platelet induction in MEG-01s cells,³⁰ was spiked to initiate the platelet production in culture (Figure 6D).

We hypothesized that O-GlcNAcylation mediates platelet production via c-Myc. To test this possibility, we establish a stable clone of c-Myc knockdown (MYCi) MEG-01s cells, where O-GlcNAcylation could be later manipulated. Notably, we could not establish a stable clone of MYCi MEG-01 cells, possibly because MEG-01 cells may be more mature than MEG-01s cells and are primed for PLP induction and could not be clonally expanded once c-Myc is knockdown. Thiamet G (0-20 μM) was used to induce cellular hyper-O-GlcNAcylation to investigate whether platelet induction by c-Myc inhibition would be abolished. Figure 6E reveals that an addition of thiamet G to the TPA-treated MYCi cells significantly reduced the

CD41a⁺ and CD42b⁺ PLPs to the similar level as those of TPA-treated CTLi cells in correspond to an increase in c-Myc level upon thiamet G treatment (Supporting Information Figure S12), supporting the critical role of O-GlcNAcylation in the regulation of c-Myc and its effect on platelets. Given that c-Myc stability is regulated by ubiquitin-mediated proteasomal degradation and that O-GlcNAcylation could interfere with other PTMs, we analyzed the influence of O-GlcNAcylation on c-Myc ubiquitination using co-immunoprecipitation. Figure 6F shows that OGT inhibition and subsequent reduction of c-Myc O-GlcNAcylation by OSMI-1 dose-dependently induced c-Myc ubiquitination in MEG-01 cells (see also Supporting Information Figure S13), indicating that O-GlcNAcylation of c-Myc regulates its stability in MBs.

3.8 | Inhibition of OGT and c-Myc causes perturbation of cell adhesion

To gain a novel insight into the potential mechanisms underlying platelet regulation by O-GlcNAcylation, we compared the genome-wide transcription profiles of MEG-01 cells with decreased O-GlcNAcylation (OGTi) and its control (CTLi) counterpart using RNA sequencing. We identified 428 DEGs between OGTi and CTLi cells, of which 248 genes were upregulated and 178 genes were downregulated (Supporting Information Figure S14A). Gene ontology (GO) and enrichment analysis was performed using DAVID.^{31,32} Figure 7A reveals cell adhesion and focal adhesion as top-ranked biological process and cellular component, thus strongly suggesting the involvement of cell adhesion in the process. The GO terms with respect to molecular function were mainly associated with binding activity, with protein binding at the top rank. As O-GlcNAcylation is a critical PTM,^{6,33} its strong effect on binding or interaction with other partners is not unexpected. Furthermore, the protein-protein interaction of DEGs that linked to the cell adhesion (GO:0007155) obtained from DAVID were subjected to network analysis with STRING

FIGURE 6 Platelet production in MBs is mediated by O-GlcNAc/c-Myc regulatory axis. A, (upper) Western blot analysis of c-Myc in OSMI-1 (5 μM) or thiamet G (TG; 10 μM)-treated cells after 10 days of MK differentiation from CD34⁺ HSPCs (day 10) and (lower) their quantitative analysis by densitometry. Data are mean ± SD (n = 3) from three independent experiments. *P < .05 vs nontreated control (CTL) cells at day 10; two-sided Student's *t* test. B, MB MEG-01 and MEG-01s cells were knocked down for c-Myc using shRNA against MYC (MYCi) and c-Myc level was evaluated by Western blotting prior to use. C, Flow cytometric analysis of CD41a⁺ and CD42b⁺ cells and PLPs in MYCi and CTLi MEG-01 cells collected at 3 days of culture. Percentage of CD41a⁺ and CD42b⁺ cells from total events (upper) and PLPs from total positive events (lower) were plotted. Data are mean ± SD (n = 3) from three independent experiments. *P < .05 vs CTLi cells; two-sided Student's *t* test. D, MYCi and CTLi MEG-01s cells were treated with or without TPA (0.1 μM) for 3 days and percentage of CD41a⁺ and CD42b⁺ cells (upper) and PLPs (lower) were evaluated by flow cytometry and plotted. Data are mean ± SD (n = 6) from six independent experiments. *P < .05 vs CTLi cells; one-way ANOVA with Bonferroni posttest. #P < .05 vs TPA-treated CTLi cells; one-way ANOVA with Bonferroni posttest. E, MYCi MEG-01s cells were similarly treated with TPA (0.1 μM) for 3 days in the presence or absence of thiamet G (TG; 5-20 μM) and percentage of CD41a⁺ and CD42b⁺ PLPs were evaluated by flow cytometry and plotted. Data are mean ± SD (n = 5) from five independent experiments. *P < .05 vs CTLi cells treated with TPA alone; NS, not significance vs CTLi cells treated with TPA alone; one-way ANOVA with Bonferroni posttest. #P < .05 vs MYCi cells treated with TPA alone; one-way ANOVA with Bonferroni posttest. F, Analysis of c-Myc ubiquitination and O-GlcNAcylation in MEG-01 cells in the presence or absence of OSMI-1 (0-20 μM) at 3 hours. All cells were treated with MG132 (50 μM) to prevent proteasomal degradation of c-Myc and cell lysates were prepared and immunoprecipitated using anti-c-Myc antibody or IgG (negative control). Flow through fraction was detected for c-Myc to confirm the pull down of c-Myc in IP fraction and β-actin for loading control (see also Supporting Information Figure S13 for quantitative analysis)

together with the identified significant players in the present study, that is, *OGT*, *YAP1* and *MYC* (Supporting Information Figure S14B).

To elaborate the platelet regulation through *O*-GlcNAc/*c*-Myc axis, the network illustrating downregulated (*blue*) and upregulated (*red*) genes was recreated based on the first and second neighbors of

OGT and *MYC* nodes (Figure 7B). We conducted qPCR on the associated genes, including *OGT*, *MYC*, *CDH2*, *CD34*, *CD99*, *ITGB7*, *ITGA4*, *ITGAL*, *ITGAM*, and *ITGAV* in *OGTi* and *MYCi* cells comparing to *CTLi* cells. Figure 7C indicates that the expression for all downregulated genes, except for *ITGAM*, were consistent between RNA sequencing

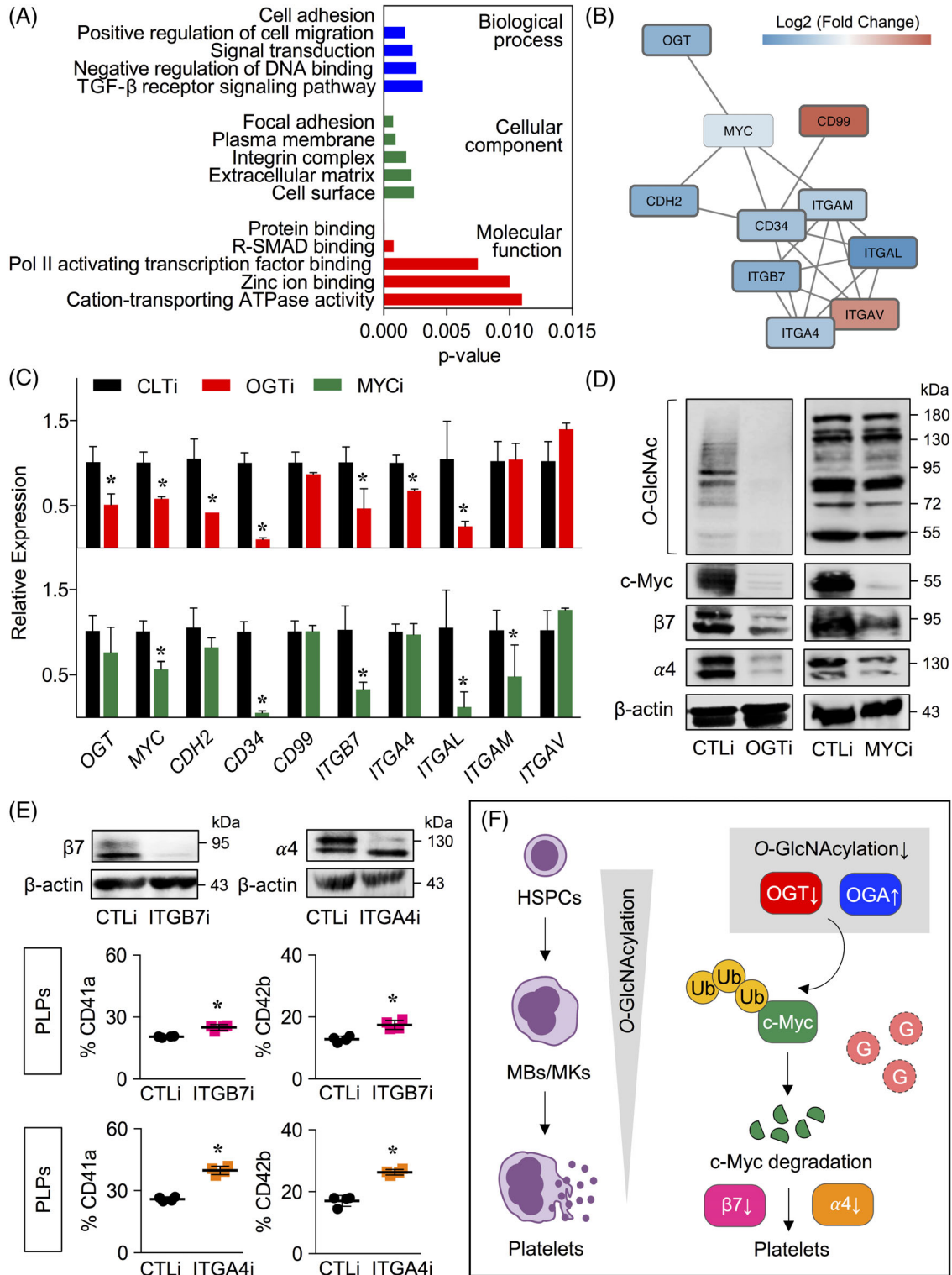


FIGURE 7 Legend on next page.

and qPCR, though we did not observe any significant changes in the expression of upregulated genes. In MYCi cells, qPCR analysis revealed the remarkable downregulation of *CD34*, *ITGB7*, and *ITGAM* when compared with CTLi cells. It has been reported that *CD34* expression on megakaryocytic lineage is limited to the early progenitor MBs,³⁴ and hence the downregulation of *CD34* in both OGTi and MYCi cells further supported the greater maturation of these cells than the control cells. Considering that *ITGAL* was barely detectable (Ct > 40 cycles), we further explored the potential contributions of integrin- β 7 and integrin- α 4 in the regulatory process.

To substantiate whether these changes were seen at posttranslational level, the level of integrin- β 7 and integrin- α 4 in OGTi cells was evaluated by Western blotting. Figure 7D shows a large decrease in integrin- β 7 and integrin- α 4 level upon inhibition of O-GlcNAcylation and its subsequently inhibition of c-Myc in OGTi cells. It is noteworthy that a tremendous reduction of c-Myc level in OGTi cells, which is less than 2-fold *MYC* downregulation (Figure 7C and D), further supported its additional regulation by O-GlcNAcylation at posttranslational level. A similar decrease in both integrin- β 7 and integrin- α 4 level upon inhibition of c-Myc in MYCi cells, despite its minimal effect on *ITGA4*, suggests that integrin- α 4 was mediated by c-Myc merely at the posttranslational level. CRISPR/Cas9 inhibition of integrin- α 4 (*ITGA4i*) and, to a lesser extent, integrin- β 7 (*ITGB7i*) induced the release of PLPs from MEG-01 cells when compared with control, supporting that integrin- β 7 and integrin- α 4 could be involved in the platelet production under O-GlcNAc/c-Myc regulatory axis.

4 | DISCUSSION

In this study, we present the novel regulatory role of metabolic sensor O-GlcNAcylation in megakaryopoiesis and thrombopoiesis. We reveal for the first time that O-GlcNAcylation plays a part throughout early and late MK differentiation and maturation. The first hint about the role of O-GlcNAcylation in the process came from the finding that O-GlcNAcylation is initially high in HSPCs, then gradually declines along the course of differentiation. Inhibition of O-GlcNAcylation via OGT provokes early MKPs, leading to the improved differentiation and

subsequent platelet production. In MB cell lines, inhibition of O-GlcNAcylation induces cellular maturation and platelets that plausibly produced through the ruptures of cytoplasm, phenotypically comparable to those of known inducers VPA and TPA.

To date, there are >1500 identified protein targets of O-GlcNAcylation, participating in the regulation of nearly all aspects of cellular processes through changes in protein function, gene expression and cellular signaling.^{35,36} Increasing evidence demonstrate the critical roles of O-GlcNAcylation in development and differentiation, including hematopoiesis. O-GlcNAcylation has been shown to be essential in T-cell development, as depletion of *Ogt* in T cells in vivo leads to a block of T cell progenitor self-renewal.³⁷ Likewise, depletion of *Ogt* in pre-B cells reduces mature B-cell survival and causes severe defects in an activation of BCR signaling.³⁸ Recent study reported that prolonged OGA inhibition impairs GATA-1-mediated erythroid differentiation in mouse erythroblasts through the disruption of transcriptional program.³⁹ Herein, we observed that OGT inhibition by OSMI-1 treatment at the initiation of MK differentiation caused a prolonged decrease in O-GlcNAcylation, of which promotes the acquisition of MBs/MKs from human-derived HSPCs, in concomitant with a decrease in c-Myc level. To support this notion, TPO, an essential cytokine for megakaryopoiesis, also downregulates c-Myc in HSPCs.^{40,41} Likewise, inhibition of OGT and O-GlcNAcylation in MBs/MKs induces platelets in an inverse correlation to c-Myc level. We validated herein that c-Myc is a key regulator of platelet production from MBs/MKs under the control of O-GlcNAcylation.

A significant increase in megakaryopoiesis and platelet count has earlier been described in c-Myc-deficient mice.⁴¹ Increasing evidence indicates that excess c-Myc diminishes platelet yield from human induced pluripotent stem cell-derived MKs.^{19,42} Our data indicate that O-GlcNAcylation regulates c-Myc stability in MBs/MKs, which is mediated through ubiquitin-mediated proteasomal degradation, consistent with previous reports in lung carcinoma.^{20,43} The counteraction of O-GlcNAcylation and ubiquitination has been increasingly reported, namely in circadian rhythm proteins BMAL1 and CLOCK,⁴⁴ apoptotic protein tBid⁴⁵ and cell cycle regulator cyclin D1,⁴⁶ although an enhanced ubiquitination upon increasing of O-GlcNAcylation was also observed in the other reports.^{20,47} We additionally found that

FIGURE 7 Inhibition of OGT and c-Myc affects cell adhesion network. Genome-wide transcription profiles of MBs upon inhibition of OGT (OGTi) were compared with control (CTLi) MEG-01 cells by RNA sequencing. A, Gene ontology (GO) and enrichment analysis of top-ranked affected biological process, cellular component, and molecular function. B, Interaction network analysis based on differentially expressed genes that linked to GO term cell adhesion (GO:0007155) and were first and second neighbors of *OGT* and *MYC* nodes. Blue and red indicate downregulated and upregulated genes, respectively, while node border width indicates the significant adjusted *P*-value. C, qPCR analysis of mRNA expression of associated genes from the network in OGTi (upper) and MYCi (lower) cells in comparison to CTLi MEG-01 cells. Data are mean \pm SD (*n* = 3) from independent experiments. **P* < .05 vs CTLi cells. D, Western blot analysis of O-GlcNAcylation, c-Myc, integrin- β 7 (β 7) and integrin- α 4 (α 4) in OGTi and MYCi cells. E, CRISPR/Cas9 system was used to repress *ITGB7* and *ITGA4* in MB MEG-01 cells, designated as *ITGB7i* and *ITGA4i* cells, respectively. (upper) Western blot analysis of integrin- β 7 and integrin- α 4 in *ITGB7i* and *ITGA4i* cells in comparison to CTLi cells. Flow cytometric analysis of CD41a⁺ and CD42b⁺ PLPs in *ITGB7i* (middle) and *ITGA4i* (lower) cells collected at 3 days of culture in comparison to CTLi cells. Percentage of CD41a⁺ and CD42b⁺ PLPs from total positive events were plotted. Data are mean \pm SD (*n* = 4) from four independent experiments. **P* < .05 vs CTLi cells; two-sided Student's *t* test. F, A schematic working model for the regulation of MK differentiation and platelet production by O-GlcNAc/c-Myc axis. Inhibition of O-GlcNAcylation, which also occurs spontaneously during MK differentiation, downregulates c-Myc at posttranslational level via the promotion of ubiquitin-proteasomal degradation, leading to the release of platelets that might involve the perturbation of integrin- β 7 and integrin- α 4. Ub, ubiquitination; G, O-GlcNAcylation

O-GlcNAcylation regulates c-Myc level in part through YAP, as YAP forms a feedback loop that regulates O-GlcNAcylation (Supporting Information Figure S15). Using GO and enrichment analysis for RNA sequencing, we identified integrin- $\beta 7$ and integrin- $\alpha 4$ as the downstream targets of O-GlcNAc/c-Myc regulatory axis of platelet production, as schematically summarized in Figure 7F. The roles of integrins in platelets are better known in platelet activation and function that signal through the shift of integrin- $\alpha 2b/\beta 3$ from a low to high-affinity state.⁴⁸ Our study suggests for the first time the involvement of other integrins in platelet release, which requires further investigation.

5 | CONCLUSION

Overall, the evidence presented here demonstrates the significance of O-GlcNAc/c-Myc axis in regulating megakaryopoiesis and thrombopoiesis. Our novel findings provide a significant basic knowledge that could be important in understanding hematologic disorders whose etiology are related to impaired platelet production and may lay groundwork for clinical applications toward an ex vivo platelet production for transfusion.

ACKNOWLEDGMENTS

We would like to acknowledge Professors Yon Rojanasakul, Davor Solter, and Barbara Knowles for their comments on the manuscript. This work was supported by grants from Thailand Research Fund/National Research Council of Thailand (RSA62080103, to S.L.) and the Commission on Higher Education (CHE-RES-RG-49, to S.I.). We thank Sirinart Buasamrit for her assistance with laboratory management and administration.

CONFLICT OF INTEREST

The authors declared no potential conflicts of interest.

AUTHOR CONTRIBUTIONS

S.L.: conception and design, financial support, collection and/or assembly of data, data analysis and interpretation, manuscript writing, final approval of manuscript; J.P.: collection and/or assembly of data, data analysis and interpretation, final approval of manuscript; P.K.: collection and/or assembly of data, final approval of manuscript; X.K.: collection and/or assembly of data, data analysis and interpretation, final approval of manuscript; K.T.: collection and/or assembly of data, final approval of manuscript; S.I.: financial support, provision of study material or patients, manuscript writing, final approval of manuscript.

DATA AVAILABILITY STATEMENT

RNA sequencing data are available at GEO under accession number: GSE150880. Other data that support the findings of this study are available on request from the corresponding author.

ORCID

Sudjit Luanpitpong  <https://orcid.org/0000-0002-1639-4935>

REFERENCES

- Ito K, Ito K. Hematopoietic stem cell fate through metabolic control. *Exp Hematol*. 2018;64:1-11.
- Goode DK, Obier N, Vijayabaskar MS, et al. Dynamic gene regulatory networks drive hematopoietic specification and differentiation. *Dev Cell*. 2016;36:572-587.
- Gautier EF, Ducamp S, Leduc M, et al. Comprehensive proteomic analysis of human erythropoiesis. *Cell Rep*. 2016;16:1470-1484.
- Miranda MB, Johnson DE. Signal transduction pathways that contribute to myeloid differentiation. *Leukemia*. 2007;21:1363-1377.
- Oburoglu L, Tardito S, Fritz V, et al. Glucose and glutamine metabolism regulate human hematopoietic stem cell lineage specification. *Cell Stem Cell*. 2014;15:169-184.
- Bond MR, Hanover JA. A little sugar goes a long way: the cell biology of O-GlcNAc. *J Cell Biol*. 2015;208:869-880.
- Józwiak P, Forma E, Brys M, Krzeslak A. O-GlcNAcylation and metabolic reprogramming in cancer. *Front Endocrinol (Lausanne)*. 2014;5:145.
- Yu M, Cantor AB. Megakaryopoiesis and thrombopoiesis: an update on cytokines and lineage surface markers. *Methods Mol Biol*. 2012;788:291-303.
- Oburoglu L, Romano M, Taylor N, Kinet S. Metabolic regulation of hematopoietic stem cell commitment and erythroid differentiation. *Curr Opin Hematol*. 2016;23:198-205.
- Popov N, Wanzel M, Madiredjo M, et al. The ubiquitin-specific protease USP28 is required for MYC stability. *Nat Cell Biol*. 2007;9:765-774.
- Machlus KR, Italiano JE Jr. From megakaryocyte development to platelet formation. *J Cell Biol*. 2013;201:785-796.
- Kishore V, Eliason JF, Matthew HW. Covalently immobilized glycosaminoglycans enhance megakaryocyte progenitor expansion and platelet release. *J Biomed Mater Res A*. 2011;96:682-692.
- Holmsen H. Physiological functions of platelets. *Ann Med*. 1989;21:23-30.
- Takeuchi K, Satoh M, Kuno H, Yoshida T, Kondo H, Takeuchi M. Platelet-like particle formation in the human megakaryoblastic leukaemia cell lines, MEG-01 and MEG-01s. *Br J Haematol*. 1998;100:436-444.
- Dhenge A, Kuhikar R, Kale V, Limaye L. Regulation of differentiation of MEG01 to megakaryocytes and platelet-like particles by Valproic acid through Notch3 mediated actin polymerization. *Platelets*. 2019;30:780-795.
- Wilson A, Murphy MJ, Oskarsson T, et al. C-Myc controls the balance between hematopoietic stem cell self-renewal and differentiation. *Genes Dev*. 2004;18:2747-2763.
- Delgado MD, León J. Myc roles in hematopoiesis and leukemia. *Genes Cancer*. 2010;1:605-616.
- Takayama N, Nishimura S, Nakamura S, et al. Transient activation of c-MYC expression is critical for efficient platelet generation from human induced pluripotent stem cells. *J Exp Med*. 2010;207:2817-2830.
- Nakamura S, Takayama N, Hirata S, et al. Expandable megakaryocyte cell lines enable clinically applicable generation of platelets from human induced pluripotent stem cells. *Cell Stem Cell*. 2014;14:535-548.
- Luanpitpong S, Angsutararux P, Samart P, Chanthra N, Chanvorachote P, Issaragrisil S. Hyper-O-GlcNAcylation induces cisplatin resistance via regulation of p53 and c-Myc in human lung carcinoma. *Sci Rep*. 2017;7:10607.
- Itkonen HM, Minner S, Guldvik IJ, et al. O-GlcNAc transferase integrates metabolic pathways to regulate the stability of c-MYC in human prostate cancer cells. *Cancer Res*. 2013;73:5277-5287.
- Lee DH, Kwon NE, Lee WJ, et al. Increased O-GlcNAcylation of c-Myc promotes pre-B cell proliferation. *Cell*. 2020;9:158.
- Meng Z, Moroishi T, Guan KL. Mechanisms of Hippo pathway regulation. *Genes Dev*. 2016;30:1-17.

24. Peng C, Zhu Y, Zhang W, et al. Regulation of the Hippo-YAP pathway by glucose sensor O-GlcNAcylation. *Mol Cell*. 2017;68:591-604.
25. Milton CC, Grusche FA, Degoutin JL, et al. The Hippo pathway regulates hematopoiesis in *Drosophila melanogaster*. *Curr Biol*. 2014;24:2673-2680.
26. Lorthongpanich C, Jiamvoraphong N, Supraditaporn K, Klaihmon P, U-pratya Y, Issaragrisil S. The Hippo pathway regulates human megakaryocytic differentiation. *Thromb Haemost*. 2017;117:116-126.
27. Zhang X, Qiao Y, Wu Q, et al. The essential role of YAP O-GlcNAcylation in high-glucose-stimulated liver tumorigenesis. *Nat Commun*. 2017;8:15280.
28. Nishimoto M, Uranishi K, Asaka MN, et al. Transformation of normal cells by aberrant activation of YAP via cMyc with TEAD. *Sci Rep*. 2019;9:10933.
29. Choi W, Kim J, Park J, et al. YAP/TAZ initiates gastric tumorigenesis via upregulation of MYC. *Cancer Res*. 2018;78:3306-3320.
30. Ogura M, Morishima Y, Okumura M, et al. Functional and morphological differentiation induction of a human megakaryoblastic leukemia cell line (MEG-01s) by phorbol diesters. *Blood*. 1988;72:49-60.
31. Huang DW, Sherman BT, Lempicki RA. Systematic and integrative analysis of large gene lists using DAVID bioinformatics resources. *Nat Protoc*. 2009;4:44-57.
32. Huang DW, Sherman BT, Lempicki RA. Bioinformatics enrichment tools: paths toward the comprehensive functional analysis of large gene lists. *Nucleic Acids Res*. 2009;37:1-13.
33. Rauth M, Freund P, Orlova A, et al. Cell metabolism control through O-GlcNAcylation of STAT5: a full or empty fuel tank makes a big difference for cancer cell growth and survival. *Int J Mol Sci*. 2019;20:1028.
34. Tang G, Wang SA, Menon M, Dresser K, Woda BA, Hao S. High-level CD34 expression on megakaryocytes independently predicts an adverse outcome in patients with myelodysplastic syndromes. *Leuk Res*. 2011;35:766-770.
35. Hahne H, Sobotzki N, Nyberg T, et al. Proteome wide purification and identification of O-GlcNAc-modified proteins using click chemistry and mass spectrometry. *J Proteome Res*. 2013;12:927-936.
36. Ong Q, Han W, Yang X. O-GlcNAc as an integrator of signaling pathways. *Front Endocrinol (Lausanne)*. 2018;9:599.
37. Swamy M, Pathak S, Grzes KM, et al. Glucose and glutamine fuel protein O-GlcNAcylation to control T cell self-renewal and malignancy. *Nat Immunol*. 2016;17:712-720.
38. Wu JL, Chiang MF, Hsu PH, et al. O-GlcNAcylation is required for B cell homeostasis and antibody responses. *Nat Commun*. 2017;8:1854.
39. Zhang Z, Parker MP, Graw S, et al. O-GlcNAc homeostasis contributes to cell fate decisions during hematopoiesis. *J Biol Chem*. 2019;294:1363-1379.
40. Yoshihara H, Arai F, Hosokawa K, et al. Thrombopoietin/MPL signaling regulates hematopoietic stem cell quiescence and interaction with the osteoblastic niche. *Cell Stem Cell*. 2007;1:685-697.
41. Guo Y, Niu C, Breslin P, et al. c-Myc-mediated control of cell fate in megakaryocyte-erythrocyte progenitors. *Blood*. 2009;114:2097-2106.
42. Gekas C, Graf T. Induced pluripotent stem cell-derived human platelets: one step closer to the clinic. *J Exp Med*. 2010;207:2781-2784.
43. Luanpitpong S, Rodboon N, Samart P, et al. A novel TRPM7/O-GlcNAc axis mediates tumour cell motility and metastasis by stabilising c-Myc and caveolin-1 in lung carcinoma. *Br J Cancer*. 2020;123:1289-1301. <https://doi.org/10.1038/s41416-020-0991-7>.
44. Li MD, Ruan HB, Hughes ME, et al. O-GlcNAc signaling entrains the circadian clock by inhibiting BMAL1/CLOCK ubiquitination. *Cell Metab*. 2013;17:303-310.
45. Luanpitpong S, Chanthra N, Janan M, et al. Inhibition of O-GlcNAcase sensitizes apoptosis and reverses bortezomib resistance in mantle cell lymphoma through modification of truncated Bid. *Mol Cancer Ther*. 2018;17:484-496.
46. Masclaf L, Dehennaut V, Mortuaire M, et al. Cyclin D1 stability is partly controlled by O-GlcNAcylation. *Front Endocrinol (Lausanne)*. 2019;10:106.
47. Srikanth B, Vaidya MM, Kalraiya RD. O-GlcNAcylation determines the solubility, filament organization, and stability of keratins 8 and 18. *J Biol Chem*. 2010;285:34062-34071.
48. Nieswandt B, Varga-Szabo D, Elvers M. Integrins in platelet activation. *J Thromb Haemost*. 2009;7:206-209.

SUPPORTING INFORMATION

Additional supporting information may be found online in the Supporting Information section at the end of this article.

How to cite this article: Luanpitpong S, Poohadsuan J, Klaihmon P, Kang X, Tangkiettrakul K, Issaragrisil S. Metabolic sensor O-GlcNAcylation regulates megakaryopoiesis and thrombopoiesis through c-Myc stabilization and integrin perturbation. *Stem Cells*. 2021;39:787-802. <https://doi.org/10.1002/stem.3349>